J. Plasma Physics (2007), *vol.* 73, *part* 6, *pp.* 901–910. © 2007 Cambridge University Press
doi:10.1017/S0022377807006368 First published online 13 February 2007 Printed in the United Kingdom

Small-amplitude electrostatic solitary waves in a dusty plasma with variable charge resonant trapped dust particles

LEILA AIT GOUGAM, MOULOUD TRIBECHE and FAWZIA MEKIDECHE

Faculty of Sciences-Physics, Theoretical Physics Laboratory, University of Bab-Ezzouar, USTHB, B.P. 32, El Alia, Algiers 16111, Algeria

(Received 2 November 2006, accepted 20 November 2006)

Abstract. Small-amplitude electrostatic solitary waves are investigated in unmagnetized dusty plasmas with variable charge resonant trapped dust particles. It is found that under certain conditions spatially localized structures, the height and nature of which depend sensitively on the plasma parameters, can exist. The effects of dust grain temperature, equilibrium dust charge, trapping parameter, and dust size on the properties of these solitary waves are briefly discussed. A neural network with a given architecture and learning process, and which may be useful to interpret experimental data, is outlined. Our investigation may be taken as a prerequisite for the understanding of the solitary dust waves that may occur in space as well as in laboratory plasmas.

1. Introduction

Ionized gases with dispersed dust grains (micrometre to sub-micrometre sized solid particles), referred to as dusty plasmas, occur in a wide variety of cosmic and terrestrial environments. Dust is an ubiquitous component of space and astrophysical environments, occurring for example in planetary rings, comets, the Earth's ionosphere, interstellar molecular clouds, and circumstellar disks [1–3]. Dust also occurs in laboratory plasmas, including those used for materials processing [4]. Waves in dusty plasmas have been studied theoretically for about two decades, beginning with the work of Bliokh and Yarashenko [5] on electrostatic waves in Saturn's rings. Dusty plasmas are known to support a wide variety of ultra-low-frequency wave modes [6–9]. The most well studied of such modes are the so-called dust-acoustic wave (DAW) [10] and dust ion-acoustic wave (DIAW) [11]. The DIAW is the usual ion-acoustic mode modified by the presence of dust particles and the DAW arises because of the restoring force provided by the plasma thermal pressure while the inertia is due to the dust mass. The DAW/DIAW propagate as linear normal modes when the phase velocity is much larger than the dust thermal velocity. However, there are numerous processes via which unstable modes can saturate and attain large amplitude [12–19]. When the amplitudes of the waves are sufficiently large, nonlinearities cannot be ignored. The nonlinearities come from the harmonic generation involving the fluid advection, the nonlinear Lorentz force, the trapping of particles in the wave potential, the ponderomotive force, etc.

https://doi.org/10.1017/S0022377807006368 Published online by Cambridge University Press

The nonlinearities in plasmas contribute to the localization of waves, leading to different and interesting nonlinear coherent structures (solitary structures, shock waves, vortices, etc.). These coherent structures may play a role of basic nonlinear elements in phenomena such as turbulence, heating, transport, etc., and hence their properties are of fundamental interest. Nonlinear DAWs and DIAWs of large and small amplitude have been studied extensively in recent years [20–44]. These analyses have been derived on the basis of the Sagdeev quasi-potentials or the reductive perturbation theory which leads to the dynamical system being described by the Korteweg–de Vries (KdV) or derivative nonlinear Schrödinger (NLS) equations. The soliton results from the balance of two effects which are the necessary ingredients to obtain soliton solutions for a nonlinear wave: nonlinearity gives rise to a process that leads to the well-known wave steepening phenomena. The wave steepening, if not stopped by some other physical phenomena, leads to wave breaking. The dispersion prevents the wave breaking and it is thereby stopped.

The aim of the present paper is to show the existence and formation of small-amplitude electrostatic solitary potentials in a charge varying dusty plasma with trapped dust particles. These nonlinear localized structures are small-amplitude, self-consistent solutions of the Vlasov equation representing saturated states of a three-stream unstable collisionless dusty plasma. The saturation is provided by an interplay between dust particle trapping and dust charging. The inclusion of the dust charge dynamics effects leads to a considerable increase in the richness and variety of the wave motions that can exist in a plasma. It also affects the nature of particle–wave interactions. This paper is organized as follows. In the next section, we present the basic equations of our theoretical model. A small-amplitude analysis is carried out in Sec. 3. The results are presented and discussed in Sec. 4. A summary of our results and conclusions are given in Sec. 5.

2. Theoretical model

We consider an unmagnetized dusty plasma having electrons, positive ions, and dust grains of density $n_{\mathrm{e}}, n_{\mathrm{i}}$, and n_{d}, respectively. We assume for simplicity that all the grains have the same charge, equal to $q_{\mathrm{d}} = -eZ$, with Z positive for negatively charged dust and negative for positively charged dust. All the dust grains are assumed to have the same size and to be spheres of radius r. On the dust timescale, the electrons and ions are assumed to be in thermal equilibrium with densities

$$n_j = n_{j0} \exp\left(-\frac{q_j \phi}{T_j}\right), \tag{1}$$

where $j = \mathrm{e}, \mathrm{i}$ denote electrons and ions, respectively, ϕ is the electrostatic potential, $q_{j=\mathrm{e,i}} = \mp e$ are the charges, and T_j the temperatures. The subscript 0 stands for equilibrium values. The dust particles are described by the coupled set of Vlasov–Poisson equations, which we solve by using the second procedure as given in [45]. Accordingly, in order to solve the Vlasov equation for dust particles with variable charge, we make use of an appropriate ansatz in terms of the constants of motion. To model the hot dust distribution in the presence of trapped particles, we refer to an appropriate Bernstein–Greene–Kruskal (BGK) solution. A BGK solution is considered to be adequate if it represents the nonlinear version of the natural eigenmodes of the plasma. Since the dust charge is allowed to change, we rewrite

https://doi.org/10.1017/S0022377807006368 Published online by Cambridge University Press

$E_{\rm d}$ as

$$E_{\rm d} = \frac{1}{2} m_{\rm d} v_{\rm d}^2 + \chi = \frac{1}{2} m_{\rm d} v_{\rm d}^2 + \int_0^{\phi} q_{\rm d}\, d\phi \tag{2}$$

so that $E_{\rm d}$ becomes a constant of the motion and thus $f(E_{\rm d})$ satisfies the stationary Vlasov equation. It is easy to show that

$$\frac{d\chi}{dx} = q_{\rm d} \frac{d\phi}{dx}. \tag{3}$$

We employ a vortex-like dust distribution function of Schamel [45] which solves the dust Vlasov equation. Thus, we have

$$f_{\rm d} = f_{\rm df} + f_{\rm dt} \tag{4}$$

with

$$f_{\rm df}(x, v_{\rm d}) = n_{\rm d0} \left(\frac{m_{\rm d}}{2\pi T_{\rm df}} \right)^{1/2} \times \exp\left(- \frac{m_{\rm d} v_{\rm d}^2/2 - e \int_0^{\phi} Z\, d\phi}{T_{\rm df}} \right) \quad \text{for } |v_{\rm d}| \succ \sqrt{\frac{2e \int_0^{\phi} Z\, d\phi}{m_{\rm d}}}, \tag{5}$$

$$f_{\rm dt}(x, v_{\rm d}) = n_{\rm d0} \left(\frac{m_{\rm d}}{2\pi T_{\rm df}} \right)^{1/2} \times \exp\left(- \beta \frac{m_{\rm d} v_{\rm d}^2/2 - e \int_0^{\phi} Z\, d\phi}{T_{\rm df}} \right) \quad \text{for } |v_{\rm d}| \preceq \sqrt{\frac{2e \int_0^{\phi} Z\, d\phi}{m_{\rm d}}}, \tag{6}$$

where the subscript f (t) represents the free (trapped) dust contribution. Here β is a parameter determining the number of trapped dust grains and its magnitude is defined as the ratio of the free hot dust temperature $T_{\rm df}$ to the hot trapped dust temperature $T_{\rm dt}$, i.e. $|\beta| = T_{\rm df}/T_{\rm dt}$. The introduction of the parameter β allows for a different temperature in the Maxwellian distribution for the trapped dust grains, $\beta = 0$ ($\beta = 1$) corresponding to a flat-topped (Maxwellian) dust distribution. Note that a hole in the trapped region, corresponding to an underpopulation of trapped dust particles, is represented by negative β terms (a vortex-like excavated trapped dust distribution). It may be noted here that the distribution function (4), as presented above, is continuous at the transition point between free and trapped particles and satisfies the regularity requirements for an admissible BGK solution. The slope of the trapped dust distribution function in velocity space is finite. With distribution (4) we obtain for $\beta < 0$

$$n_{\rm d}(\phi) = \int_{-\infty}^{+\infty} f_{\rm d}(x, v_{\rm d})\, dv_{\rm d} = n_{\rm d0} \left\{ \exp\left(- \frac{\chi}{T_{\rm df}} \right) \operatorname{erfc}\left(\sqrt{-\frac{\chi}{T_{\rm df}}} \right) + \frac{2}{\sqrt{-\pi\beta}} W\left(\sqrt{\beta \frac{\chi}{T_{\rm df}}} \right) \right\}, \tag{7}$$

where $W(x)$ is the Dawson integral, namely $W(x) = \exp(-x^2) \int_0^x \exp(t^2)\, dt$. Poisson's equation then becomes for $\beta < 0$

$$\frac{d^2\Psi}{dX^2} = \exp(\Psi) - f \exp(-\sigma\Psi) + \frac{(f-1)}{Q_{\rm d0}} Q_{\rm d} N_{\rm d}, \tag{8}$$

https://doi.org/10.1017/S0022377807006368 Published online by Cambridge University Press

where

$$N_{\rm d} = n_{\rm d}/n_{\rm d0} = \exp(-\gamma\xi)\ \mathrm{erfc}\ (\sqrt{-\gamma\xi}) + \frac{2}{\sqrt{-\pi\beta}} W(\sqrt{\beta\gamma\xi}) \tag{9}$$

and $f = n_{\rm i0}/n_{\rm e0}$, $\sigma = T_{\rm e}/T_{\rm i}$, and $\gamma = rT_{\rm e}^2/e^2T_{\rm df}$. The normalized quantities

$$\Psi = \frac{e\phi}{T_{\rm e}}, \quad \xi = \frac{e^2}{rT_{\rm e}^2}\chi, \quad X = \frac{x}{\lambda_{\rm De}}, \quad Q_{\rm d} = \frac{eq_{\rm d}}{rT_{\rm e}}$$

are introduced and $\lambda_{\rm De} = (T_{\rm e}/4\pi n_{\rm e0}e^2)^{1/2}$ is the electron Debye length. Normalization of (3) yields

$$\frac{d\xi}{dX} = Q_{\rm d}\frac{d\Psi}{dX}. \tag{10}$$

Charge neutrality at equilibrium requires $n_{\rm e0} - n_{\rm i0} + Z_0 n_{\rm d0} = 0$.

In the standard orbit-limited probe model for the dust grain [46] the latter is charged by the plasma currents at the grain surface. The charging current originates from electrons and ions hitting the grain surface. Accordingly, the variable dust charge $q_{\rm d} = -eZ$ is determined self-consistently by (note that we consider a one-dimensional stationary plasma)

$$v_{\rm d}\frac{dq_{\rm d}}{dx} = I_{\rm e} + I_{\rm i}, \tag{11}$$

where $I_{\rm e}$ and $I_{\rm i}$ are, respectively, the average microscopic electron and ion currents entering the dust grains. The grain current from the Boltzmann electrons and ions are [47–49]

$$I_j = \pi r^2 q_j (8T_j/\pi m_j)^{1/2} n_j W_j, \tag{12}$$

where $r \ll \lambda_{\rm De}$ is the grain radius, and m_j are the masses. For $q_{\rm d} < 0$, we have [50,51]

$$W_{\rm e} = \exp(eq_{\rm d}/rT_{\rm e}) \tag{13}$$

and

$$W_{\rm i} = 1 - eq_{\rm d}/rT_{\rm i}. \tag{14}$$

We assume that the cold dust grains, whose mass is much greater than that of the ions, are accelerated by a weak pre-sheath field to a velocity $v_{\rm d0}$. Thus the number conservation equation, after integration, yields

$$n_{\rm d}v_{\rm d} = n_{\rm d0}v_{\rm d0}. \tag{15}$$

After rearranging the terms in (11), one can obtain the normalized charging equation

$$\frac{dQ_{\rm d}}{dX} = kN_{\rm d}\left\{-\exp(\Psi + Q_{\rm d}) + \sqrt{\frac{\mu}{\sigma}} f \exp(-\sigma\Psi)(1 - \sigma Q_{\rm d})\right\} \tag{16}$$

with k given by

$$k = \sqrt{\frac{2n_{\rm e0}e^2r^2}{m_{\rm e}v_{\rm d0}^2}} \tag{17}$$

and $\mu = m_{\rm e}/m_{\rm i}$. Equation (16) is the additional dynamical equation that is coupled to the plasma equations through the plasma currents. The dust electric charge becomes a dynamical variable which is coupled self-consistently to the other dynamical variables such as density and potential. Charge neutrality at equilibrium

https://doi.org/10.1017/S0022377807006368 Published online by Cambridge University Press

($\Psi = 0$) requires the following constraint:

$$f = \sqrt{\frac{\sigma}{\mu}} \frac{\exp(Q_{\mathrm{d}0})}{1 - \sigma Q_{\mathrm{d}0}}. \tag{18}$$

In the following numerical simulation, the value of f is deduced from the above relation while the other remaining parameters ($Q_{\mathrm{d}0}, r, T_{\mathrm{e}}, \sigma, T_{\mathrm{df}}, \beta, \mu, n_{\mathrm{i}0}$ and $v_{\mathrm{d}0}$) are given first.

3. Small-amplitude analysis

We note that the characteristic time for dust motion is of the order of tens of milliseconds for micrometre sized grains, while the dust charging time is typically of the order of 10^{-8} s. Within the time of charging, the displacement of the grain is thus negligible compared with the spatial scale of the problem. It follows that the charging process can be treated as a local phenomenon, and the convective term on the left-hand side of (11) can be neglected. It follows that we have

$$I_{\mathrm{e}} + I_{\mathrm{i}} \simeq 0 \tag{19}$$

and the grains are always at the floating potential. Thus, (16) and (18) lead to

$$(1 + \sigma)\Psi = \ln\left\{ \frac{1 - \sigma Q_{\mathrm{d}}}{1 - \sigma Q_{\mathrm{d}0}} \exp(Q_{\mathrm{d}0} - Q_{\mathrm{d}}) \right\}. \tag{20}$$

Neglecting terms of $O(\sigma^{-1})$ we obtain the following transcendental relation between Ψ and Q_{d}:

$$\sigma\Psi = Q_{\mathrm{d}0} - Q_{\mathrm{d}} + \ln \frac{Q_{\mathrm{d}}}{Q_{\mathrm{d}0}}. \tag{21}$$

Assuming that the relative variation of the charge is sufficiently small and expanding

$$\ln \frac{Q_{\mathrm{d}}}{Q_{\mathrm{d}0}} \simeq (Q_{\mathrm{d}} - Q_{\mathrm{d}0})/Q_{\mathrm{d}0} \tag{22}$$

we obtain

$$\frac{Q_{\mathrm{d}}}{Q_{\mathrm{d}0}} = 1 - \frac{\sigma\Psi}{Q_{\mathrm{d}0} - 1} \tag{23}$$

and it becomes possible to rewrite (8) as

$$\frac{d^2\Psi}{dX^2} = -\frac{dV(\Psi)}{d\Psi}, \tag{24}$$

where $V(\Psi)$ represents the pseudo-potential. Multiplying both sides of (8) by $d\Psi/dX$ and integrating once we obtain the quadrature

$$\frac{1}{2}\left(\frac{d\Psi}{dX}\right)^2 + V(\Psi) = 0, \tag{25}$$

where the Sagdeev potential for our purpose reads as

$$V(\Psi) = -\exp(\Psi) - \frac{f}{\sigma}\exp(-\sigma\Psi) - \frac{(f-1)}{Q_{\mathrm{d}0}} \int_0^{\Psi} Q_{\mathrm{d}} N_{\mathrm{d}}\, d\Psi \tag{26}$$

with

$$Q_{\mathrm{d}} N_{\mathrm{d}} = Q_{\mathrm{d}0}\left(1 - \frac{\sigma\Psi}{Q_{\mathrm{d}0} - 1}\right)\left\{ \exp(-\gamma\xi)\ \mathrm{erfc}\ (\sqrt{-\gamma\xi}) + \frac{2}{\sqrt{-\pi\beta}} W(\sqrt{\beta\gamma\xi}) \right\}$$

https://doi.org/10.1017/S0022377807006368 Published online by Cambridge University Press

and

$$\xi = \int_0^{\Psi} Q_{\rm d}\, d\Psi = Q_{\rm d0}\left[\Psi - \frac{\sigma\Psi^2}{2(Q_{\rm d0}-1)}\right]. \tag{27}$$

Equation (25) can be regarded as an 'energy integral' of an oscillating particle of unit mass, with a velocity $d\Psi/dX$ and position Ψ in a potential $V(\Psi)$. In this limit, $\Psi \ll 1$, the nature of the solution of (25) may be obtained explicitly. Expanding in Ψ and retaining leading-order terms, we find that (9) and (26) reduce respectively to

$$N_{\rm d} = 1 - \gamma Q_{\rm d0}\Psi + \frac{4(1-\beta)}{3\sqrt{\pi}}\gamma Q_{\rm d0}\sqrt{-\gamma Q_{\rm d0}}\Psi^{3/2} + \frac{\gamma Q_{\rm d0}}{2}\left(\frac{\sigma}{Q_{\rm d0}-1} + \gamma Q_{\rm d0}\right)\Psi^2 + O(\Psi^{5/2}) \tag{28}$$

and

$$V(\Psi) = A_1\Psi^2 + A_2\Psi^{5/2} + O(\Psi^3), \tag{29}$$

where

$$A_1 = \frac{1}{2}\left\{(f-1)\gamma Q_{\rm d0} + \frac{(f-1)\sigma}{Q_{\rm d0}-1} - 1 - f\sigma\right\},$$
$$A_2 = \frac{8(\beta-1)}{15\sqrt{\pi}}(f-1)\gamma Q_{\rm d0}\sqrt{-\gamma Q_{\rm d0}}. \tag{30}$$

Performing the last step in deriving soliton solutions, namely solving the 'energy equation' (25), one obtains

$$\Psi(X) = \left(2\frac{A_1}{A_2}\right)^2 \operatorname{sech}^4\left[\sqrt{-\frac{A_1}{8}}X\right]. \tag{31}$$

Solution (31) represents a small-amplitude stationary solitary wave provided

$$\frac{f-1}{1+f\sigma}\left(\gamma Q_{\rm d0} + \frac{\sigma}{Q_{\rm d0}-1}\right) < 1. \tag{32}$$

The potential from (31) deviates from that of the usual KdV soliton given by

$$\Psi(X) = \Psi_M \operatorname{sech}^2\left[\sqrt{\frac{1}{6}\Psi_M}X\right] \tag{33}$$

in the power and the scaling of the sech argument. Prior to the numerical investigation, it may be instructive to further distinguish between (31) and (33). To this end, we propose here to use a neural network with a given architecture and learning process outlined in [52] to which the reader is referred. In Figs 1 and 2, we illustrate the evolution of $\mathrm{Log}_2(\lambda_i)$ for both (33), see Fig. 1, and (31), see Fig. 2. In the trapped dust free case (Fig. 1), the evolution of λ_i exhibits a very interesting and unexpected result. A merging tendency between λ_1, λ_2, and λ_3 occurs, as recently reported in [52]. This tendency to merge disappears in the presence of trapped dust particles as hinted in Fig. 2 where the λ_i terms, after some iterative growing, level off at constant values (although it seems that this is not always the case and a precise choice of the initial values of the λ_i terms must be made). This may be attributed to the saturation provided by an interplay between dust charging and dust trapping. One can then make an analogy with the work of Buti [53], who showed that even a small fraction of charged dust grains can eliminate the chaos in non-dissipative

https://doi.org/10.1017/S0022377807006368 Published online by Cambridge University Press

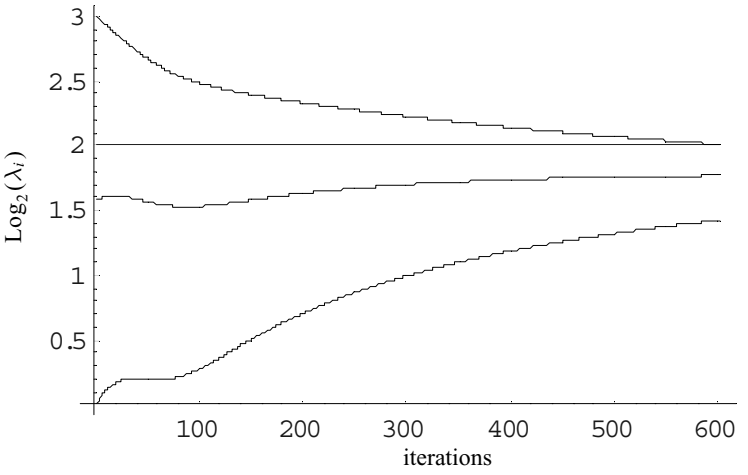


Figure 1. Plot of $\mathrm{Log}_2(\lambda_i)$ versus the number of iterations in the case $F(X) = 2\ \mathrm{sech}^2(X/10)$.

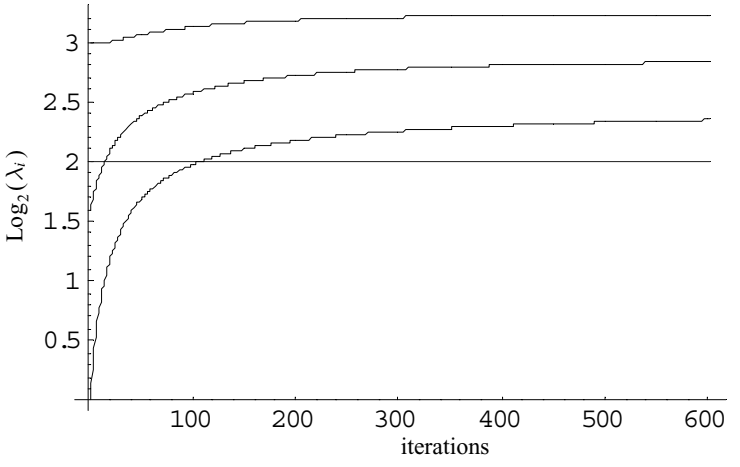


Figure 2. Plot of $\mathrm{Log}_2(\lambda_i)$ versus the number of iterations in the case $F(X) = 2\ \mathrm{sech}^4(X/10)$.

Alfvénic systems. Experimentally (where Ψ is not known analytically but a precise set of data can be generated), the occurrence (or absence) of merging may allow us to draw an important conclusion regarding the existence (or not) of resonant trapped particles. We recall that flat topped electron distributions, characteristic of the presence of trapped electrons, are generally observed in ion-acoustic wave experiments.

4. Numerical analysis

For the sake of comparison, we have plotted the spatial variation of Ψ for various values of β in Fig. 3. The electrostatic potential Ψ exhibits a spatially localized structure as can be checked easily from the structure of the Sagdeev potential

https://doi.org/10.1017/S0022377807006368 Published online by Cambridge University Press

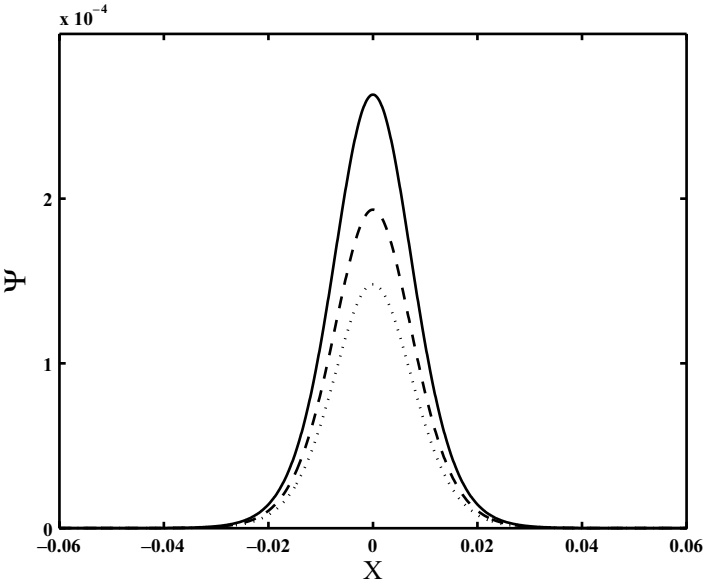


Figure 3. Small-amplitude soliton solution for the electrostatic potential Ψ for different values of $\beta = -0.2$ (solid line), -0.4 (dashed line), and -0.6 (dotted line) with $T_e = 2$ eV, $r = 1$ μm, $\sigma = 3$, $Q_{d0} = -1.4$, $n_{i0} = 10^8$ cm^{-3}, and $T_{df} = T_i/5$. The value of f deduced from (18) is 3.51.

$V(\Psi)$ (29). The parameters $T_e = 2$ eV, $r = 1$ μm, $Q_{d0} = -1.4$, $n_{i0} = 10^8$ cm^{-3}, $\sigma = 3$, and $T_{df} = T_i/5$ have been chosen so that the conditions for the existence of soliton solutions are fulfilled. It can be seen that as $|\beta|$ increases the height of the soliton decreases, whereas its width is found to be insensitive to β. With a decrease of $|Q_{d0}|$ (Fig. 4) (the charge of the dust grain becomes less negative) the amplitude of the soliton is enhanced while the width of it is narrowed, i.e. a decrease of the net negative charge residing on the grain surface makes the solitary structure more spiky. Now by retaining terms up to Ψ^3 (26) may be expanded as

$$V(\Psi) = A_1\Psi^2 + A_2\Psi^{5/2} + A_3\Psi^3 + O(\Psi^{7/2}), \tag{34}$$

where

$$A_3 = -\frac{\sigma(f-1)\gamma Q_{d0}}{2(Q_{d0}-1)} - \frac{(f-1)\gamma Q_{d0}}{6} - \frac{1-f\sigma^2}{6}. \tag{35}$$

5. Summary and conclusion

To conclude, we have addressed the problem of small-amplitude electrostatic solitary structures in a dusty plasma with vortex-like variable charge dust distribution. Our results show that in such a plasma spatially localized structures, the height and nature of which depend sensitively on the plasma parameters, can exist. However, their stability is far from easy to prove. We have then limited ourselves to finding localized structure solutions producing indirect evidence of their possible realization. The effects of dust grain temperature, equilibrium dust charge, trapping parameter, and dust size on the properties of these solitary waves have been discussed. At present, we do not have any experimental observations of solitary waves in dusty plasmas with variable charge trapped dust particles to

https://doi.org/10.1017/S0022377807006368 Published online by Cambridge University Press

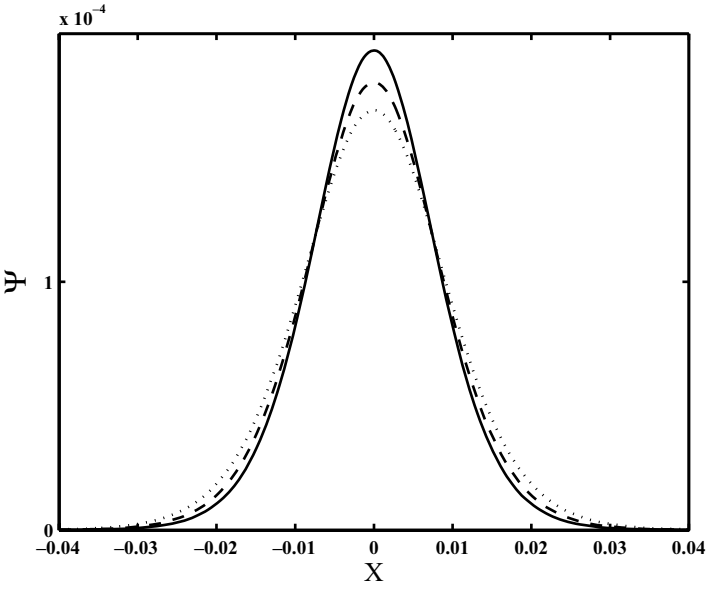


Figure 4. Small-amplitude soliton solution for the electrostatic potential Ψ for different values of $Q_{d0} = -1.4$ (solid line, $f = 3.51$), -1.5 (dashed line, $f = 3.01$), and -1.6 (dotted line, $f = 2.58$) with $T_e = 2$ eV, $r = 1$ μm, $\sigma = 3$, $n_{i0} = 10^8$ cm^{-3}, $\beta = -0.4$, and $T_{df} = T_i/5$.

compare with our theoretical predictions. However, considering the wide relevance of nonlinear oscillations in laboratory and space dusty plasmas, our investigation may be taken as a prerequisite for the understanding of the solitary waves that may occur in space and laboratory plasmas. It may be stressed here that the time evolution and stability analysis of these nonlinear dust solitary waves are problems of great importance but beyond the scope of the present work.

Acknowledgements

The third author wishes to thank B. G. Giraud (Service de Physique Théorique, DSM, CE Saclay) for his hospitality and very helpful suggestions. This work was supported in part by the Ministère de l'Enseignement Supérieur et de la Recherche Scientifique Contracts Nos. D1602/04/03 and D1602/17/04.

References

[1] Goertz, C. K. 1989 *Rev. Geophys.* **27**, 271.
[2] Mendis, D. A. and Rosenberg, M. 1994 *Annu. Rev. Astron. Astrophys.* **32**, 419.
[3] Horanyi, M. 1996 *Annu. Rev. Astron. Astrophys.* **34**, 383.
[4] Selwyn, G. S. 1993 *Japan. J. Appl. Phys.* **32**, 3068.
[5] Bliokh, P. V. and Yarashenko, V. V. 1985 *Sov. Astron* **29**, 330 (in English).
[6] Verheest, F. 2000 *Waves in Dusty Space Plasmas*. Dordrecht: Kluwer.
[7] Shukla, P. K. and Mamun, A. A. 2002 *Introduction to Dusty Plasma Physics*. Bristol: IOP, and references therein.
[8] Shukla, P. K. 2001 *Phys. Plasmas* **8**, 1791.
[9] Merlino, R. L., Barkan, A., Thompson, C. and D'Angelo, N. 1998 *Phys. Plasmas* **5**, 1607.
[10] Rao, N. N., Shukla, P. K. and Yu, M. Y. 1990 *Planet. Space Sci.* **38**, 543.
[11] Shukla, P. K. and Silin, V. P. 1992 *Phys. Scripta* **45**, 508.

https://doi.org/10.1017/S0022377807006368 Published online by Cambridge University Press

[12] Mamun, A. A. and Gebreel, A. A. 2000 *Eur. Phys. J.* D. **10**, 301.
[13] Shukla, P. K. and Stenflo, L. 2000 *Phys. Plasmas* **7**, 2738.
[14] Shukla, P. K., Stenflo, L. and Morfill, G. M. 2001 *IEEE Trans. Plasma Sci*. **29**, 198.
[15] Shukla, P. K., Stenflo, L., Mamun, A. A., Resendes, D. P. and Sorasio, G. 2002 *J. Geophys. Res*. **107**, 1293.
[16] Shukla, P. K. and Mamun, A. A. 2003 *Phys. Lett.* A **313**, 424.
[17] Shukla, P. K. and Eliasson, B. 2004 *Phys. Plasmas* **11**, 584.
[18] Shukla, P. K. and Mamun, A. A. 2004 *Phys. Plasmas* **11**, 1233.
[19] Tribeche, M., Ait Gougam, L. and Aoutou, K. 2006 *Phys. Plasmas* **13**, 092105.
[20] Mamun, A. A., Cairns, R. A. and Shukla, P. K. 1996 *Phys. Plasmas* **3**, 702.
[21] Mamun, A. A., Cairns, R. A. and Shukla, P. K. 1996 *Phys. Plasmas* **3**, 2610.
[22] Shchekinov, Y. A. 1997 *Phys. Lett.* A **225**, 117.
[23] Ma, J. X. and Liu, J.-Y. 1997 *Phys. Plasmas* **4**, 253.
[24] Tagare, S. G. 1997 *Phys. Plasmas* **4**, 3167.
[25] Mamun, A. A. 1998 *J. Plasma Phys*. **59**, 575.
[26] Mamun, A. A., Alam, M. N. and Azad, A. K. 1998 *Phys. Plasmas* **5**, 1212.
[27] Kakati, M. and Goswami, K. S. 1998 *Phys. Plasmas* **5**, 4508.
[28] Mamun, A. A. 1999 *Astrophys. Space Sci*. **268**, 443.
[29] Mamun, A. A. 1999 *Astrophys. Space Sci*. **260**, 507.
[30] Mamun, A. A., Russell, S. M., Mendoza-Briceño, C. A., Alam, M. N., Datta, T. K. and Das, A. K. 2000 *Planet. Space Sci*. **48**, 163.
[31] Mendoza-Briceño, C. A., Russell, S. M. and Mamun, A. A. 2000 *Planet. Space Sci*. **48**, 599.
[32] Das, G. C., Sarma, J. and Roychoudhury, R. 2001 *Phys. Plasmas* **8**, 74.
[33] Shukla, P. K. and Mamun, A. A. 2001 *IEEE Trans. Plasma Sci*. **29**, 221.
[34] Farid, T., Mamun, A. A., Shukla, P. K. and Mirza, A. M. 2001 *Phys. Plasmas* **8**, 1529.
[35] Ghosh, S., Sarkar, S., Khan, M. and Gupta, M. R. 2001 *IEEE Trans. Plasma Sci*. **29**, 409.
[36] Mamun, A. A. and Shukla, P. K. 2001 *Phys. Lett.* A **290**, 173.
[37] Mamun, A. A. and Shukla, P. K. 2002 *Phys. Scripta* **98**, 107.
[38] Mamun, A. A. and Shukla, P. K. 2002 *Geophys. Res. Lett*. **29**, 1870.
[39] Mamun, A. A. and Shukla, P. K. 2002 *Phys. Plasmas* **9**, 1468.
[40] Ghosh, S., Sarkar, S., Khan, M. and Gupta, M. R. 2002 *Phys. Plasmas* **9**, 1150.
[41] Mamun, A. A. and Shukla, P. K. 2002 *IEEE Trans. Plasma Sci*. **30**, 720.
[42] Popel, S. I., Golub, A. P., Losseva, T. V., Ivlev, A. V., Khrapak, S. A. and Morfill, G. 2003 *Phys. Rev.* E **67**, 056402.
[43] El-Labany, S. K., El-Taibany, W. F., Mamun, A. A. and Moslem, W. M. 2004 *Phys. Plasmas* **11**, 926.
[44] Li, Yang-fang, Ma, J. X. and Li, Jing-ju 2004 *Phys. Plasmas* **11**, 1366.
[45] Schamel, H. 1986 *Phys. Rep*. **140**, 161.
[46] Chen, F. F. 1965 *Plasma Diagnostic Techniques* (ed. R. H. Huddlestone and S. L. Leonard). New York: Academic, ch. 4.
[47] Barnes, M. S., Keller, J. H., Forster, J. C., O'Neill, J. A. and Coultas, D. K. 1992 *Phys. Rev. Lett*. **68**, 313.
[48] Ma, J. X. and Yu, M. Y. 1995 *Phys. Plasmas* **2**, 1343.
[49] Whipple, E. C. 1981 *Rep. Prog. Phys*. **44**, 1198.
[50] Ma, J. X., Liu, Jin-yuan and Yu, M. Y. 1997 *Phys. Rev.* E **55**, 4627.
[51] Liu, Jin-yuan and Ma, J. X. 1997 *Phys. Plasmas* **4**, 2798.
[52] Giraud, B. G. and Touzeau, A. 2001 *Phys. Rev.* E **65**, 016109.
[53] Buti, B. 1997 *Phys. Lett.* A **235**, 241.

https://doi.org/10.1017/S0022377807006368 Published online by Cambridge University Press